ELSEVIER

Journal of Nuclear Materials 290–293 (2001) 443–447

journal of nuclear materials

www.elsevier.nl/locate/jnucmat

Local recycling coefficients and wall equilibration in tokamaks ☆

P.K. Mioduszewski [a,*], L.W. Owen [a]

[a] *Oak Ridge National Laboratory, P.O. Box 2009, Oak Ridge, TN 37831-8072, USA*

Abstract

The recycling coefficient of the first wall of a fusion device is a space- and time-dependent quantity. In present analyses, it is often taken as one single parameter, without taking account of the vast variations across the surface areas of the vessel. The present paper is an analysis of the spatially dependent recycling coefficient as a function of time, using the DIII-D vacuum vessel as an example. In the first step, an analytical formula is constructed to simulate the recycling coefficient as a function of the trapped particle flux, based on computer simulations (W. Eckstein, Calculated Trapping Curves of D in C, Si, Garching Report IPP 9/33, October 1980). In the second step, the vessel walls are subdivided into a computational grid of 123 segments and for each segment the incident particle flux during a discharge is computed with the B2 plasma and DEGAS neutral codes. The incident particle fluxes and the recycling coefficient formula are then used to analyze the local and temporal recycling behavior of the wall.

Keywords: First wall; Hydrogen trapping; Long pulse; Recycling; Wall pumping

1. Introduction

Wall recycling of hydrogen isotopes affects plasma fueling and performance on the one hand and wall pumping and inventory on the other hand [2,3]. In computational models, the recycling coefficient is often assumed to be one single coefficient, either time-dependent or constant throughout the discharge. Since the particle fluxes can vary over the vacuum vessel wall by up to five orders of magnitude, the recycling coefficients will vary correspondingly. Furthermore, since the particle fluence to the various parts of the wall evolves during a plasma discharge, the recycling coefficient evolves with the fluence or, at constant flux, with time. Hence, the actual recycling coefficient has strong spatial and temporal variations during a plasma discharge. To better understand which parts of the wall are pumping or fueling throughout the time of evolution of a discharge, we perform an analysis of the recycling coefficient as a function of location and time.

2. Recycling coefficient

To facilitate computations on wall recycling, we describe the recycling coefficient with an analytical formula to fit trapping calculations obtained with computer simulations. The amount of trapped deuterium in graphite has been computed by Eckstein [1] with the TRIM code [4] as a function of particle fluence and plasma temperature for isotropic and Maxwellian distributions between 10 and 200 eV. We construct an analytical recycling coefficient to match these calculations. The trapping rate depends on the incident particle flux $\phi_{\rm inc}$ and the recycling coefficient $R(n_{\rm tr})$, where $n_{\rm tr}$ is the number of trapped particles; it is given by

$$\frac{{\rm d}n_{\rm tr}}{{\rm d}t} = \phi_{\rm inc}[1 - {\rm R}(n_{\rm tr})]. \quad (1)$$

☆ This research was sponsored by the US Department of Energy under the contract DE-AC05-00OR-22725 with UT-Batelle LLC.

* Corresponding author. Tel.: +1-865 574 2715 fax: +1-865 574 1191.

E-mail address: mioduszewspk@ornl.gov (P.K. Mioduszewski).

0022-3115/01/$ - see front matter
PII: S0022-3115(00)00512-2

Table 1
Parameters for the tanh recycling coefficient

Energy (eV)	a	c	n_{sym} ($\times 10^{20}$ m^{-2})	δ ($\times 10^{20}$ m^{-2})
20	0.23	0.77	0.9	0.5
50	0.28	0.72	2.0	1.2
100	0.32	0.68	3.0	2.4
200	0.37	0.63	5.0	4.5

The trapped fluence dependence of the recycling coefficient is approximated with a hyperbolic tangent (tanh):

$$R(n_{tr}) = a \ \tanh\left[\frac{n_{tr} - n_{sym}}{\delta}\right] + c. \quad (2)$$

The four parameters a, c, n_{sym}, and δ are used to adjust the shape of the tanh curve. A set of parameters that provides a good match with the Eckstein curves for Maxwellian particle distributions is given in Table 1.

Assuming ϕ_{inc} = constant, the differential equation (1) is easily solved numerically. The result yields the trapped particle fluence as a function of the incident fluence or, at constant flux, as a function of time. Fig. 1 shows this dependence for four different particle energies with Maxwellian distribution. The initial values of the recycling coefficients have been adjusted to fit the Eckstein TRIM curves, which are higher for Maxwellian particles than for the corresponding mono-energetic particles. Experimentally measured trapping coefficients are typically obtained with mono-energetic particles and, therefore, are different from the curves in Fig. 1. But the tanh function has enough flexibility to adjust it to the shape of mono-energetic trapping coefficients as well. These curves are also in good agreement with the experimental curves of Haasz et al. [5].

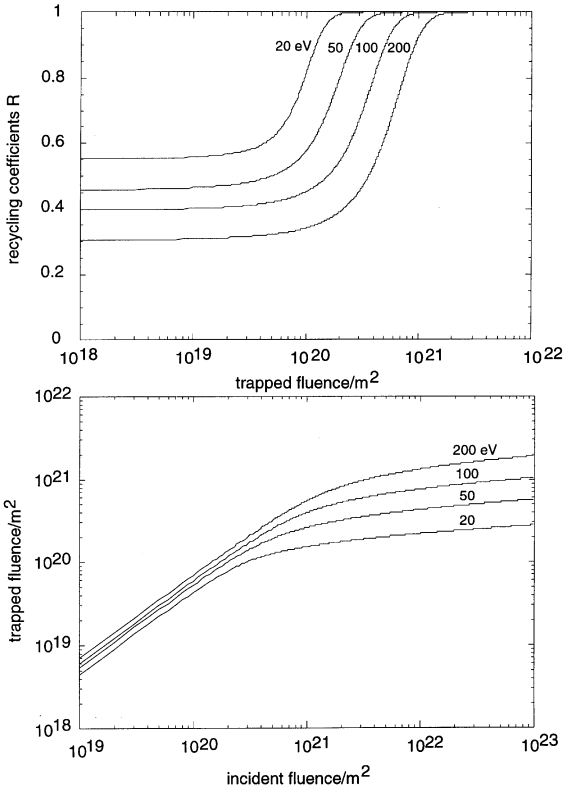

Fig. 1. (a) Number of trapped D atoms as a function of incident particle fluence; (b) recycling coefficients as a function of trapped particle fluence.

3. Computational grid of vacuum vessel segments and zones

The particle fluxes in the divertor strike zones can be up to several times 10^{23} m^{-2} s^{-1}, whereas some other parts of the wall may receive fluxes in the order of 10^{18} m^{-2} s^{-1}. Correspondingly, the local recycling will reach unity in less than 1 s or in thousands of seconds. Using a single global recycling coefficient is, therefore, not very meaningful in characterizing the wall response. Since there is usually no diagnostics which determines the particle fluxes everywhere on the first wall, another way to obtain them is to use a neutral code such as DEGAS [6] to determine the flux and energy everywhere on the wall. We have used DEGAS to determine the particle fluxes and energies incident on the wall.

For this purpose the vacuum vessel was divided into a computational grid of 123 segments. Subsequently, the boundary plasma and the particle fluxes were calculated with the B2 plasma code [7] and the DEGAS neutral code. After the calculation of the recycling coefficients for each segment, all 123 segments were grouped into five zones with similar fluxes. This subdivision of the DIII-D vacuum vessel wall is depicted in Fig. 2. The areas of the zones are: zone 1 = 24 m^2, zone 2 = 24 m^2, zone 3 = 17 m^2, zone 4 = 5.6 m^2 and zone 5 = 1.6 m^2. Zone 5 turned out to be of little importance, but was carried along to clarify the effect of the private flux zone.

As a typical example for a low-power neutral beam discharge (96740) the segment areas (a), the particle fluxes (b), and the particle energies (c), all as a function of the segment number are shown in Fig. 3.

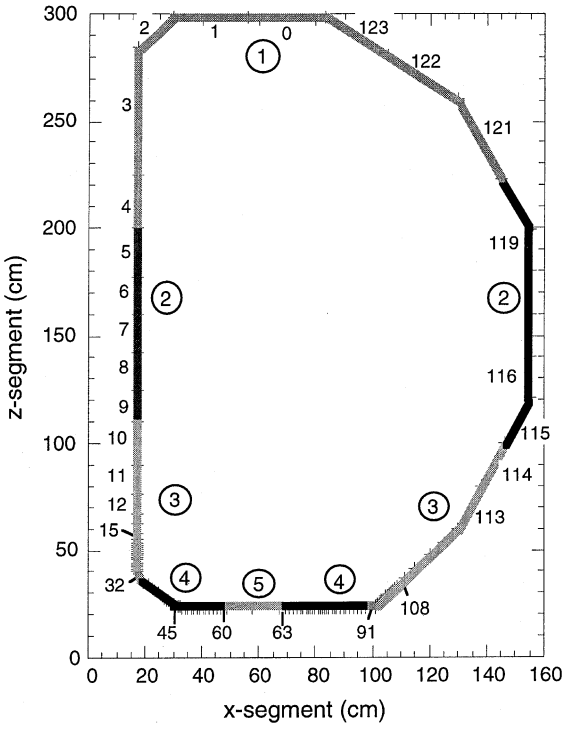

Fig. 2. DIII-D vacuum vessel with 123 segments grouped into five principal zones.

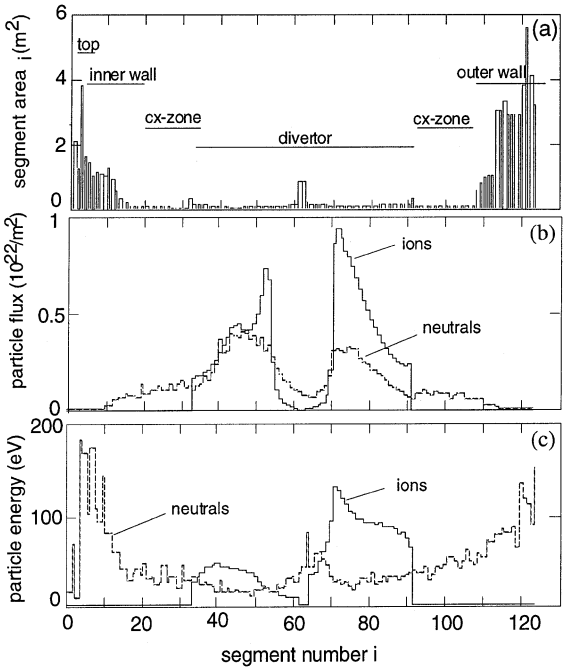

Fig. 3. (a) Distribution of segment areas as a function of segment number used for DEGAS computations; (b) ion and neutral particle fluxes as a function of segment number; (c) particle energies (Maxwellian) for each segment.

4. Computation of the trapped particle fluences

In order to calculate the fluence trapped in each segment after a given time, we combine Eqs. (1) and (2) into the following differential equations:

$$\frac{dn_{tr}}{dt} = \phi_{inc}\left(1 - \left[a \tanh\left(\frac{n_{tr} - n_{sym}}{\delta}\right) + c\right]\right) \quad (3)$$

and solve it individually for all 123 segments. In the following example, we have chosen the parameters corresponding to a particle energy of 50 eV from Table 1 and solved Eq. (3) numerically for $t = 0$–10 s and for selected segments up to 28 800 s ($= 8$ h). Since it is cumbersome to present all 123 resulting curves, we have chosen some characteristic segments from each zone, depicted in Fig. 4(a) and (b).

Fig. 4(a) shows the trapped fluences for a 10-s discharge and Fig. 4(b) shows the respective recycling coefficients. In the divertor segments (40, 49, 75, 88) most of the trapping occurred in a fraction of a second and at $t = 10$ s the maximum trapping is about 6×10^{20} m^{-2},

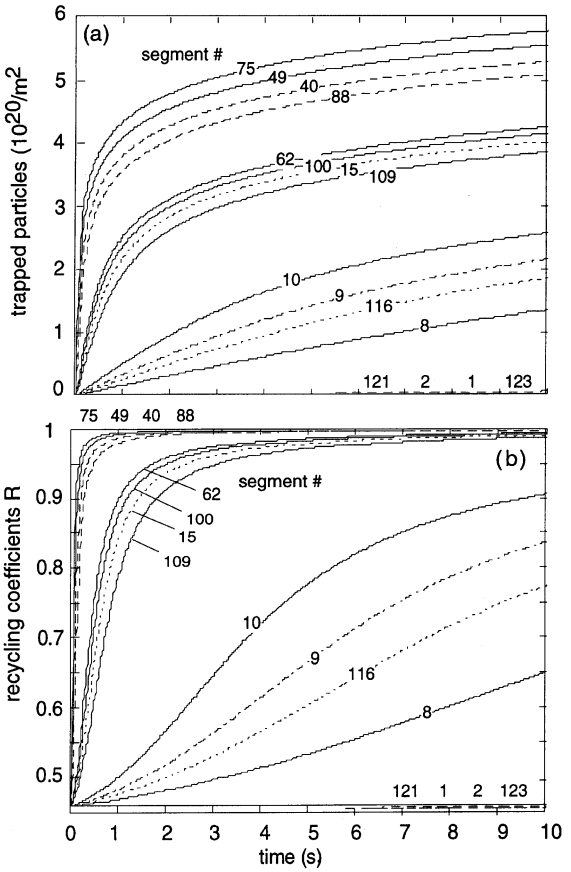

Fig. 4. (a) Trapped particle fluence for relevant segments for a 10-s discharge; (b) evolution of the recycling coefficients for the respective segments.

which corresponds to the highest value of the 50 eV curve in Fig. 1(b). The corresponding recycling coefficients approach unity in less than a second. The second group (15, 62, 100, 109) is in the private flux zone (pf-zone) and the charge-exchange zone (cx-zone). Here, most of the trapping happens within a few seconds, followed by a slow additional increase. The third group (8, 9, 10, 116) is in zone 2, around the midplane of the vessel. Due to the low flux in this area, the trapping is almost linear up to the end of the discharge. Finally, in the top of the vessel (1, 2, 121, 123) the flux is so low that the trapping here is negligible in the overall balance; the recycling coefficients remain essentially at their initial values. As we see from Fig. 3, the maximum particle flux is about 9×10^{21} m^{-2} s^{-1}, i.e. for a 5-s discharge the incident fluence is 4.5×10^{22} m^{-2} which corresponds to about 5.5×10^{20} m^{-2} trapped fluence at 50 eV as Fig. 1(b) indicates. Calculating the recycling coefficients with Eq. (2) and the trapped fluences, we get the series of curves in Fig. 4(b).

5. Pumping, recycling and wall equilibration in the principal wall zones

The four groupings of segments and trapped fluences recognized above suggest the arrangement of the segments into four zones. To evaluate the significance of the pf-zone, we carry along a fifth zone (the pf-zone) and analyze the overall recycling characteristics in terms of five principal zones.

To evaluate the dynamics of wall pumping (trapping) and the significance of the different zones, we have plotted the pumping rates and total pumped fluences for each zone for $t = 0$–10 s as log–log plots in Fig. 5(a) and (b). The pumping rate in the divertor strike zone (4) starts with 1.7×10^{22} s^{-1} ($\sim$32 Pa m^3 s^{-1}), but is surpassed in about 0.2 s by the pumping in the cx-zone (3) at 5×10^{21} s^{-1}. The pf-zone does not seem to have a significant impact at any time of the discharge. The area around the midplane (2), however, due to its large size and capacity, starts to exhibit pumping rates equal to the cx-zone at $t = 10$ s. The pumping in the top of the vessel (1) is negligible in a 10-s discharge.

Fig. 5(b) shows the accumulated fluences for each zone. As expected, the fluence in the divertor zone dominates in the beginning, but at $t = 1$ s, the cx-zone starts to surpass it. At the end of 10 s the cx-zone has accumulated the highest fluence, although it looks like zone 2 might dominate in longer-pulse discharges. To test this, we have run a 100-s discharge, but due to space limitations detailed results will be presented elsewhere. Here it may suffice to state that the trapped fluence in the midplane-zone (2) becomes equal to that in the divertor zone (4) at $t = 20$ s and gets close to that of the cx-zone (3) at $t = 100$ s. For discharges longer than 10 s,

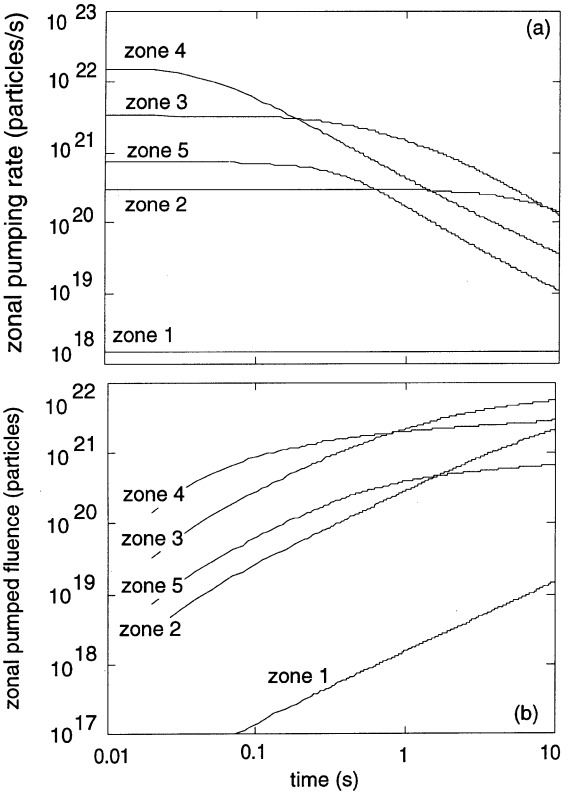

Fig. 5. (a) Total pumping rate (particles s^{-1}) for each zone; (b) the corresponding accumulated particle fluence for each zone as a function of time.

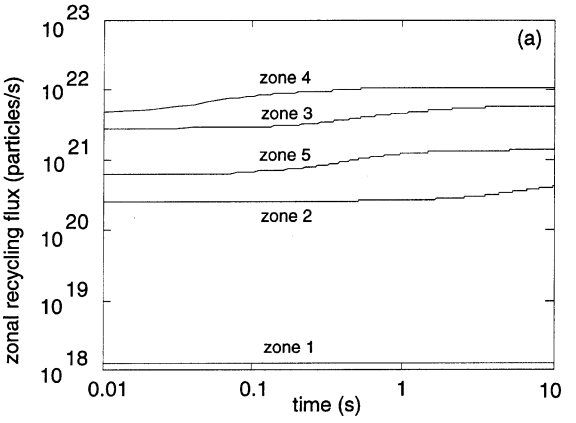

Fig. 6. Time evolution of the recycling flux emitted from each zone.

the midplane-zone becomes increasingly more important.

Finally, we have calculated the recycled flux for each zone, corresponding to the recycle fueling sources. As shown in Fig. 6(a), the total recycling flux is dominated

at all times by the divertor strike zones, although the recycling flux from the cx-zone is only a factor of two lower.

6. Summary and future work

This analysis shows that the recycling coefficient is a strong function of space and time. How does this analysis compare with experimental data? The present computations were carried out for a 50 eV particle energy and the resulting total trapped fluence matches the total gas input of about 13 Pa m^3 s^{-1} for this discharge. Repeating the computations for 100 eV particles, however, results in a total pumped fluence of 24 Pa m^3, i.e. the overall result is almost a factor of two of the above experimental value. To fine-tune the result in future work, we will add energy dependence by introducing the particle energy for each segment. Furthermore, the trapping dynamics over a sequence of discharges with intermittent outgassing will be analyzed. Finally, it should be mentioned that the present model provides a first-order analysis of time- and space-resolved recycling, whereas the processes analyzed here do not include the important effect of co-deposition on carbon walls. How this can be included, will be addressed in future work. With metal walls, however, such as beryllium or molybdenum, the present model can be used in its present form just by using the corresponding trapping curves. Although the latter may vary with surface conditions, the present model will provide a sufficiently close representation of the recycling process in a tokamak vessel.

References

[1] W. Eckstein, Calculated Trapping Curves of D in C, Si, Garching Report IPP 9/33, October 1980.
[2] J. Ehrenberg et al., J. Nucl. Mater. 162–164 (1989) 63.
[3] J. Winter, Plasm. Phys. Contr. Fus. 38 (1996) 1503–1542.
[4] L.G. Haggmark, J.P. Biersack, J. Nucl. Mater. 93&94 (1980) 664.
[5] A. Haasz et al., J. Nucl. Mater. 232 (1996) 219.
[6] D.B. Heifetz, D. Post et al., J. Comp. Phys. 46 (1982) 309.
[7] B.J. Braams, Contr. Plasma Phys. 36 (1996) 276.